Springer

Journal of Mechanical Science and Technology 23 (2009) 3132~3139

Journal of Mechanical Science and Technology

www.springerlink.com/content/1738-494x
DOI 10.1007/s12206-009-0910-6

# Effect of a blind spot in a dielectrophoretic field on the separation of human breast cancer cells (MCF 7) †

Youngho Kim[1], Jangwon Lee[1], Jaemin An[1], Sang Ho Lee[2] and Byungkyu Kim[1,*]

[1]*School of Aerospace and Mechanical Engineering, Korea Aerospace University, Goyang, Gyeonggi-do 412-791, Korea*
[2]*Laboratory of Reproductive & Developmental Biology, School of Life Sciences and Biotechnology, Korea University, 5ga-1, Anam-dong, Seongbuk-gu, Seoul 136-701, Korea*

(Manuscript Received December 5, 2008; Revised April 16, 2009; Accepted May 25, 2009)

**Abstract**

Previously, we proposed a 'dielectrophoretically activated cell sorting' (DACS) system, which can be applied to the separation of various cells without labeling them with magnetic or fluorescent materials. By using a specific frequency range, it was verified that the dielectric material properties of cells can be exploited in order to collect target cells from a cell mixture. However, because about 20% of the error in separation efficiencies was always detected, it became a subject to investigate. Therefore, we assumed that variance in cell size might be responsible for the errors. By measuring the diameter of human breast cancer cells (MCF 7) and classifying separation efficiencies according to diameter, it was verified that the errors in separation efficiency are affected by cell size. Moreover, the existence of a 'blind spot,' i.e., a space with weak force within the dielectrophoretic field generated by a pair of electrodes, was proven by commercial code CFD-ACE$^{+®}$. With simulation and experimental results, we demonstrated that some efficiency errors occur because small sized cells (between 15 and 20 μm) pass through the 'blind spot'.

***Keywords*:** Dielectrophoresis; Cell separation; DACS; MCF 7

## 1. Introduction

In the biomedical research field, microfabrication technology has provided various tools [1] for particle separation based on electric [2-4], magnetic [5-7], optical [8], hydrodynamic [9, 10], ultrasonic force [11, 12], and adhesion difference [13]. Nevertheless, most attempts at efficient manipulation of bioparticles in microchannels have proven to be more challenging.

Given its advantage in that dielectrophoresis (DEP) technology is simply and directly applicable to various platforms as a matter of convenience [14], we previously proposed a 'dielectrophoretically activated cell sorter'(DACS) [15], which was employed to separate mouse embryonic carcinoma cells (P19 EC) from red blood cells (RBCs) by using DEP. Compared to separation efficiencies, it was verified that the cells are affected by a frequency of 5 MHz under an applied voltage (sinusoidal potential of 8 $V_{p-p}$). Subsequently, we performed cell separation based on the 'frequency dependence' of human breast cancer cells (MCF 7) and normal human breast epithelial cells (MCF 10A) as one clinically meaningful application [16]. The experimental results showed that the cells are affected by a specific range of frequencies (between 34 and 36 MHz) under an applied voltage (sinusoidal potential of 8 $V_{p-p}$). On the other hand, it was also found that about 20% of the errors were consistently observed in both cases: P19 EC cells (79.4 ± 6.8 % of separation efficiency), and MCF 7 cells (77.5 ± 0.5 % of separation efficiency).

In this article, we focus on investigating the effect of cell size as the primary cause of separation errors in DACS. Basically, all of the cells used have various

† This paper was recommended for publication in revised form by Associate Editor Haecheon Choi

*Corresponding author. Tel.: +82 2 300 0101, Fax.: +82 2 3158 4429
E-mail address: bkim@kau.ac.kr

© KSME & Springer 2009

diameters according to cell cycles from G1 to M phases, which lead to fluctuations in the DEP force that acts on each cell since the DEP force is proportional to the cube of the radius of a cell (Eq. 1). Consequently, it is supposed that various cell sizes can be the main reason for separation errors. Based on the comparison of separation efficiencies according to cell size, size dependence was verified. Moreover, by calculating the distribution of the electric field in the microchannel by commercial code CFD-ACE$^{+®}$, we were able to find a 'blind spot,' i.e., a space with weak force within the dielectrophoretic field generated by the pair of electrodes. With experimental results based on the movie clip, it was demonstrated that separation errors stem from the relationship between various cell sizes and the location of the blind spot produced by disuniformity in the dielectrophoretic field.

### *1.1 Theoretical*

The dielectrophoretic force $F_{\mathrm{DEP}}$ acting on a particle depends on the following: the particle radius $r$, the DC permittivity of the liquid medium $\varepsilon_0\varepsilon_m$, the electric field gradient $\nabla E^2$, and the real value of the Clausius-Mossotti factor $K(\omega)$ in which $\omega$ is the angular frequency of the AC electric field [17, 18]. The Clausius-Mossotti factor $K(\omega)$ in Eq. (1) is given by

$$F_{DEP} = 2\pi r^3 \varepsilon_0 \varepsilon_m \,\mathrm{Re}[K(\omega)]\nabla E^2 \tag{1}$$

$$K(\omega) = \frac{\varepsilon_p^* - \varepsilon_m^*}{\varepsilon_p^* + 2\varepsilon_m^*} \tag{2}$$

$$\varepsilon_i^* = \varepsilon_0\varepsilon_i - j\frac{\sigma_i}{\omega} \tag{3}$$

The value is determined by complex AC permittivity $(\varepsilon_i)^*$. The represented index $i$ symbolizes either the particle ($i$=p) or the liquid medium ($i$=m). The complex AC permittivity is basically composed of a real part and an imaginary part inclusive of the conductivity $\sigma_i$ and the angular frequency $\omega$ of the AC electric field. The sign of the Clausius-Mossotti factor is determined according to the changes in the experimental conditions such as frequency due to the applied field as well as medium conductivity. Based on the sign, the dielectrophoretic force affects the movement of the particle, which is either repelled from (as a result of a negative DEP if the sign of the factor is negative) or attracted to (as a result of a positive DEP if the sign of the factor is positive) the designated electrode. There is, moreover, the specific frequency (the so-called cross-over frequency $f_0$) at which the DEP force acting on a homogeneous particle becomes zero. As shown in Eq. (4), it is determined by mathematical derivation using $\mathrm{Re}|K(\omega)|= 0$[19].

$$f_0 = \frac{1}{2\pi\varepsilon_0}\sqrt{\frac{\left(\sigma_p^* + 2\sigma_m\right)\left(\sigma_p^* - \sigma_m\right)}{\left(\varepsilon_p + 2\varepsilon_m\right)\left(\varepsilon_m - \varepsilon_p\right)}} \tag{4}$$

## 2. Materials and method

### *2.1 Microfabrication*

Based on the microfabrication processes previously reported [15], a DACS system was prepared. To make up for the weak points such as buffer leaking or cell clogging in the previous DACS system, two parts in the system were developed. The interface for inlet in the device was replaced with a nanoport adapter (10-32 coned Nanoport™ Assembly N-333, Upchurch Scientific®, USA), improving the interface between the tube and the device, since we experienced a great deal of leakage due to the weak bonding force between the existing PDMS layer and the glass wafer under the high pressure of a microsyringe pump. In addition, the cell stagnation and pressure build-up were eliminated by changing the shape of the inlet from a circle to an asymmetric ellipse, which reduced cell clogging in the inlet, enabling cells to transfer in the channel more stably and securely.

### *2.2 Experimental setup for cell separation*

Fig. 1 shows the experimental setup. In order to observe the movement of target cells in separation, the DACS system was mounted on an inverted microscope (IX81, Olympus Co., Japan). A micro-syringe pump (VIT-FIT, Lambda Co., Switzerland) and a microsyringe (Hamilton, 1801RN 10 ml, USA) were used for precise control of the buffer and particle streams in the microdevice. A function generator (33250A, Agilent, USA) was used to apply AC voltage (operating frequency, 10 MHz to 100 MHz; voltage, 7 $V_{p\text{-}p}$). Images of the cell separation were recorded to a PC through a CCD camera installed in the microscope.

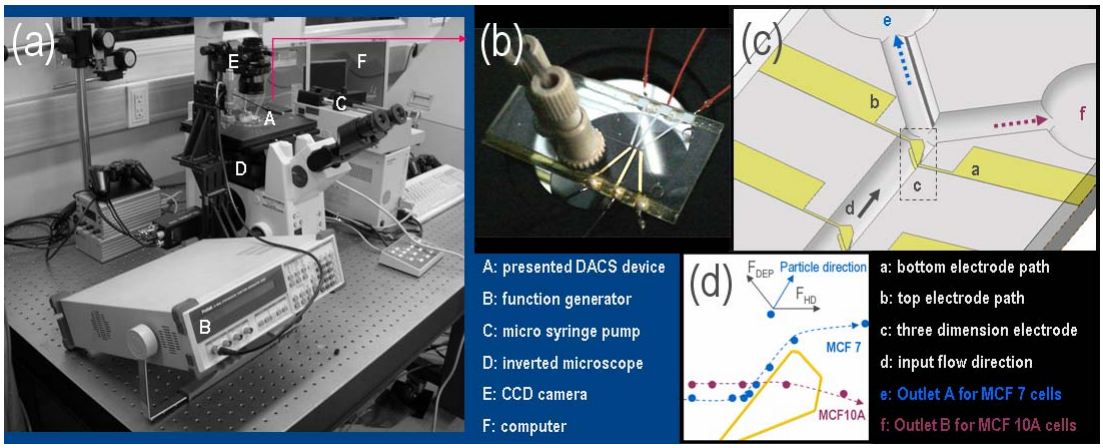


Fig. 1. Experimental setup: (a) Experimental environment, (b) DACS device, (c) structural elements of the DACS device, and d) fundamental schematic for bioparticles separation: if crossover frequency (COF) of the MCF 10A cells is employed, most of the MCF 7 cells bounce around the electrodes and move into outlet A. In contrast, other MCF 10A cells pass through the electrodes and move into outlet B. For the case of the MCF 7 (MCF 10A) cells moving into outlet B (or outlet A), we defined this as 'error.'

### *2.3 Cell preparation: MCF7 and MCF10A*

MCF10A cells as a human breast cell line and MCF 7 cells as a human breast adenocarcinoma cell line were obtained from the American Type Culture Collection (ATCC, Manasa, VA, USA). The MCF 10A cells were cultured in Dulbecco's modified essential medium (DMEM)/F-12 medium containing 5% horse serum, 100 ng $ml^{-1}$ cholera toxin, 10 ng/ml epidermal growth factor, 0.5 mg/ml hydrocortisone, and 10 mg $ml^{-1}$ insulin (all from Sigma Chemical, St Louis, MO) as described in our previous report [16] at 37ºC under an atmosphere of 5% $CO_2$. The MCF7 cells were also similarly grown in DMEM supplemented with 10% heat-inactivated fetal calf serum. When the cells confluenced about 80% after a 48-72 hour incubation period, they were handled by a brief exposure to 0.025% trypsin-EDTA solution (Invitrogen Co, CA, USA). Then after the cells were washed twice in each medium, the cells at a final concentration of $10^7$ cells $ml^{-1}$ were re-suspended in each medium including 8.5% (w/v) sucrose plus 0.3% (w/v) dextrose buffer [20].

## 3. Results and discussion

### *3.1 Cell separation with DACS*

When a 45-MHz DEP signal (7 $V_{p-p}$) was applied to the electrodes and fluid flow through the microchannel was 0.35 $\mu$ L/min, it was verified that the MCF 7 cells started to bounce and move into outlet A (Fig. 2). When a 60-MHz DEP signal (7 $V_{p-p}$) was applied to the electrodes, the bouncing pattern of the MCF 10A cells was also verified. By using the cross-over frequency of the MCF 7 cells, we assumed that the proposed DACS device enabled the separation of the MCF 7 and MCF 10A cells due to their properties of dielectric materials. To test this assumption further, the MCF 7 cells were labeled with Hoechst 33342 for 25 minutes [15] and mixed with the MCF 10A cells. After the cell mixture was separated by the DACS system, the MCF 7 and MCF 10A cells in each outlet were counted and compared statistically.

### *3.2 Separation efficiency*

Fig. 3 shows the fraction of the cells collected before and after separation. With a ratio of 1:2 (MCF 7: MCF 10A) in the cell mixture, cell separation was performed at a frequency of 45 MHz (7 $V_{p-p}$). After the separation process, each of the collected cells was counted and classified according to the place from which they were collected (outlet A or outlet B). If the total percentage of the MCF 7 cells before separation was 100%, about 84% of the MCF 7 cells after separation were collected at outlet A because of their dielectric properties. In other words, the DEP force causes them to bounce, and then enables the cells to move them into outlet A. For the case of the MCF 10A cells, compared with the total percentage

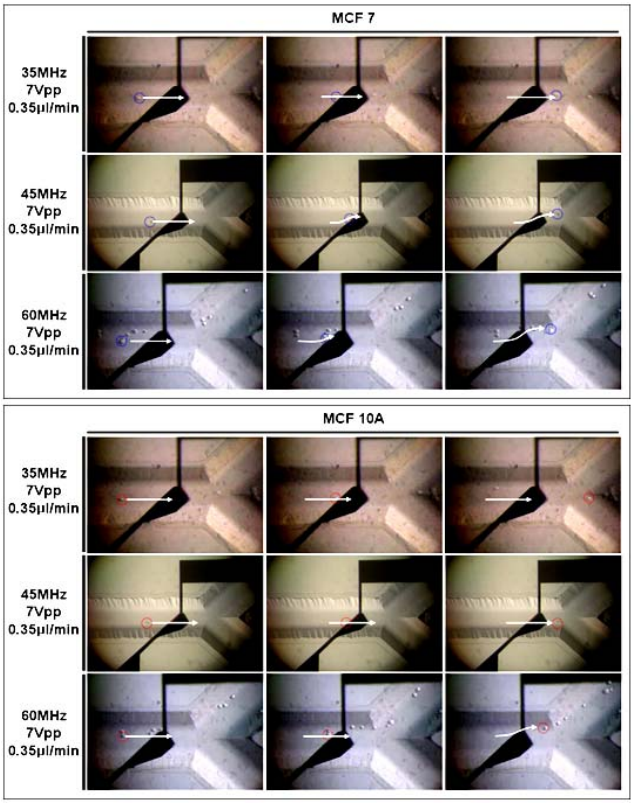


Fig. 2. Cell separation: MCF 7 and MCF 10A cells bounce at 45 and 60 MHz, respectively.

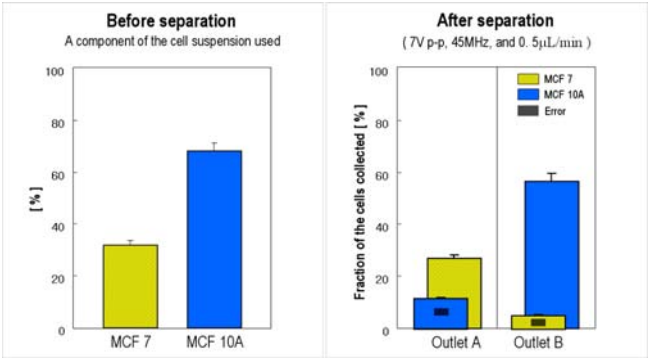


Fig. 3. Separation efficiencies of MCF 7 and MCF 10A cells before and after separation.

before separation, about 83% of the MCF 10A cells after separation were collected at outlet B since the DEP force does not act on them. Therefore, it was verified that the MCF 7 and MCF 10A cells were able to be separated. However, there is some separation error, represented by a black-colored square in Fig. 3. About 16% of the total number of MCF 7 cells was gathered at outlet B, and about 17% of the total number of MCF 10A cells was gathered at outlet A. Therefore, we hypothesized that the error might be affected by the diameter of the cells since size variation was observed while we were carrying out the separation experiment.

### *3.3 Measurement of cell size*

To investigate the effect due to the diameter of the

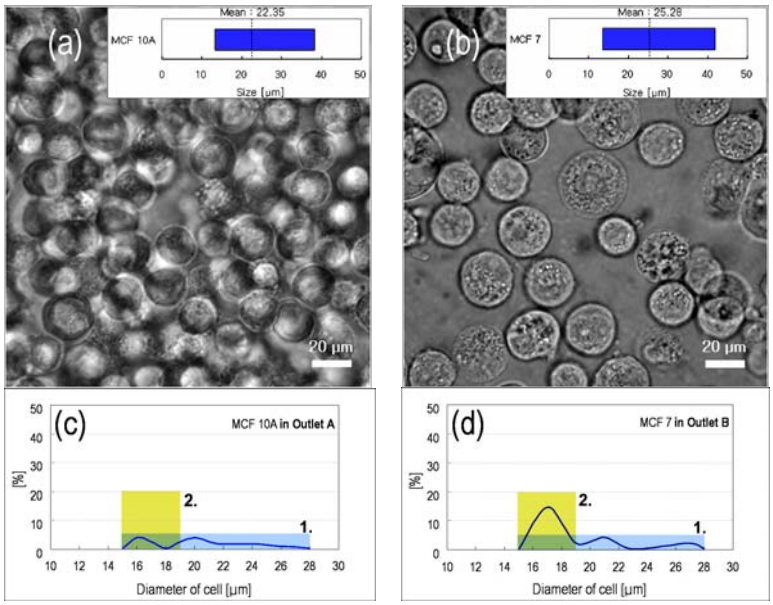


Fig. 4. Measurement of cell size and classification of separation efficiencies based on cell size. When (a) MCF 10A and (b) MCF 7 cells are suspended in buffer solution, their sizes are measured by inverted microscope (IX81, Olympus Co., Japan). In that the entire cells are included in the various cell cycles from G1 to M phases, it is possible to verify that the quantity of genetic material (DNA) packaged in cells leads to physically various sizes. (c) Proportion of MCF 10A cells in outlet A out of the total MCF 10A cells collected. (d) Proportion of MCF 7 cells in outlet B out of the total MCF 7 cells collected.

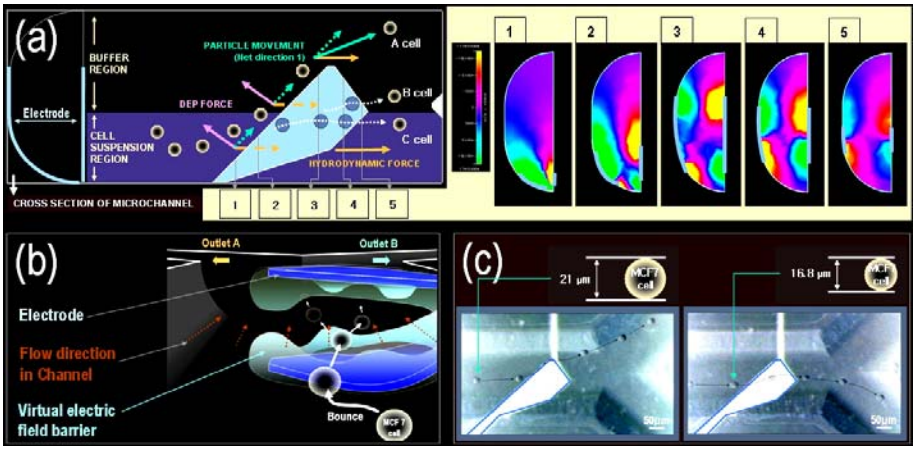


Fig. 5. Cell movement in dielectrophoretic field: (a) Deflection; particle movement is basically decided by vector summation of DEP force (by a pair of electrodes) and hydrodynamic force (by a microsyringe pump). Under the fundamentals, A cells show an ideal separation. Contrary to expectations, movement of cells such as B or C cells was occasionally found, and as a result, they are counted as one of the errors. CFD-ACE code was introduced in order to investigate the phenomenon. From the five cross-sectional images (from 1 to 5) along the electrode, the existence of a 'blind spot' within the dielectrophoretic field was verified. (b) Virtual image assembled from 25 cross-sectional images; we schematically depicted the field distribution as a 3D-electric field barrier around the pair of electrodes and the pathway; some of the MCF 7 cells pass through near the 'blind spot'. (c) Error generation based on cell size; to demonstrate our assumption, we investigated the phenomenon by using the movie clips. MCF 7 cells were traced by CCD camera, at intervals of 0.5 sec. It was verified that if the diameter of an MCF 7cell is about 21μm, it moves into outlet A. However, if the diameter of an MCF 7cell is about 16.8μm, it moves not into outlet A but outlet B. Therefore, in that the MCF 7 cells of 16.8 μm are relatively less affected by the electric field than those of 21μm, it can be said that the phenomenon is based on cell size.

cells, we measured the diameter of the cells used and statistically calculated the range. As shown in Fig. 4 (a), MCF 10A and MCF 7 cells show various shapes and sizes despite being the same kind because of their heterogeneity. From the captured images, it was confirmed that variations in the diameter of the MCF 10A and MCF 7 cells were about 25 and 27 μm, respectively. Accordingly, we concluded that the size variation of the cells used could be one reason for the error.

### *3.4 Analysis based on the diameter of the cells*

Based on the above result that the cells used have various sizes, we classified separation efficiency according to variances in cell size. Fig. 4(c) and (d) show the distribution of MCF 10A cells in outlet A and MCF 7 cells in outlet B, respectively. From the curves of separation efficiency, it was confirmed that there are two patterns. Pattern 1 is related to the fluctuation of fluid flow in the microchannel at the initial stage of the separation process since a similar pattern and magnitude are simultaneously found at outlet A and B. However, pattern 2 points to a significant finding in that the errors of the MCF 7 cells are related to their diameter. This is due to the fact that the majority of cells detected at outlet B were MCF 7 cells of small size (between 15 and 20 μm) rather than those of large size (between 22 and 28 μm). Accordingly, it is possible to say that if the diameter of the MCF 7 cells is less than about 20 μm, they might end up in outlet B.

### *3.5 Blind spot in the DEP field*

To examine why the MCF 7 cells included in the small size (between 15- and 20 μm) range were mainly detected at outlet B, we studied distribution of the electric field in the microchannel of DACS system. By analyzing the movie clips, the relationship between size and deflection of target cells was investigated. The distribution of the electric field was calculated by commercial code CFD-ACE$^{+®}$. As shown in Fig. 5(a), the dielectrophoretic field generated by the pair of electrodes has a space (or 'blind spot') with a weak DEP force. Fig. 5(b) shows a 3-dimensional structure based on the five cross-sectional images (Fig. 5(a)). From the image, we could guess that the blind spot in the dielectrophoretic field allows the small sized cells (within 20 μm) to pass through the pair of electrodes and as a result, some MCF 7 cells were found at outlet B. Accordingly, the separation error asso-ciated with the MCF 7 cells stems not only from the blind spot but also their size. To confirm this phe-nomenon, the experimental video clip was analyzed, as shown in Fig. 5(c). Based on the diameter of the cells that passed through, we found that the large-sized (between 21 to 28 μm) cells were basically deflected, while relatively small-sized (between 14 to 20 μm) cells were allowed through the electrode.

## 4. Conclusion

In our previous work, we proposed that the DACS system is applicable to cell separation. By using dielectric properties of the cells (e.g., P19 mouse embryonal carcinoma cells and red blood cells), it was verified that each of the cells could be separated with high purity (greater than 95%). For the case of cell separation using MCF 7 and MCF 10A cells, however, it was found that about 16% of the MCF 7 cells and 17% of the MCF 10A cells accumulated at each of the opposite outlets. Under the assumption that the various sizes of the cells used might affect separation efficiency, we measured the diameter of the MCF 7 and MCF 10A cells. From the fact that MCF 7 (between 14 and 41 μm) and MCF 10A cells (between 14 and 39 μm) have a similar size range, we investigated their separation efficiencies according to variances in the diameter of the cells. In that most of the MCF 7 cells detected at outlet B belonged to the small size range (between 15 and 20 μm), it is possible to conclude that variances in cell size affect their separation efficiency and error generation. Moreover, we were able to find the 'blind spot' in the dielectrophoretic field by using com-mercial code CFD-ACE$^{+®}$. From the experimental video clip images, it was significantly demonstrated that the blind spot allows small MCF 7 cells to pass through the pair of electrodes without bounce. Accordingly, we were able to confirm that the blind spot affects separation efficiency in the proposed DACS system. Important issues of the current system, such as appropriate control of the distance between electrodes and dimension of the channel to eliminate the blind spot, are to be investigated in the future. In conclusion, the current system can be widely used to separate the target cells if the blind spot according to the diameter of the target cells is controlled.

## Acknowledgements

This research was supported by the Korean Ministry of Education, Science and Technology (MEST) and the Korea Science and Engineering Foundation (KOSEP) : S. Shin under the Bio Interphase Program (Bio Tool R&D Group, Contract Number M10531020001-08N3102-00110).

## References

[1] M. Toner and D. Irimia, Blood-on-a-chip, *Annu. Rev. Biomed. Eng.* 7 (2005) 77-103.

[2] P. R. C. Gascoyne and J. Vykoukal, Particle separation by dielectrophoresis, *Electrophoresis* 23 (2002) 1973-1983.

[3] Y. Li, C. Dalton, H. J. Crabtree, G. Nilsson and K. V. I. S. Kaler, Continuous dielectrophoretic cell separation microfluidic device, *Lab Chip* 7 (2007) 239-248.

[4] A. Rosenthal, B. M. Taff and J. Voldman, Quantitative modeling of dielectrophoretic traps, *Lap Chip* 6 (2006) 508-515.

[5] M. A. M. Gijs, Magnetic bead handling on-chip: new opportunities for analytical applications *Microfluid Nanofluid* 1 (2004) 22-40.

[6] K. Han and A. B. Frazier, Paramagnetic capture mode magnetophoretic microseparator for high efficiency blood cell separations, *Lap Chip* 6 (2006) 265-273.

[7] Y. Kim, S. Hong, S. H. Lee, K. Lee, S. Yun, Y. Kang, K. Paek, B. Ju and B. Kim, Novel platform for minimizing cell loss on separation process: Droplet-based magnetically activated cell separator, *Rev. Sci. Instrum.* 78 (2007) 074301-074307.

[8] D. G. Grier, A revolution in optical manipulation, *Nature* 424 (2003) 21-27.

[9] S. Choi and J. Park, Continuous hydrophoretic separation and sizing of microparticles using slanted obstacles in a microchannel, *Lap Chip* 7 (2007) 890-897.

[10] M. Yamada and M. Seki, Microfluidic Particle Sorter Employing Flow Splitting and Recombining, *Anal. Chem.* 78 (2006) 1357-1362.

[11] A. Neild, S. Oberti, G. Radziwill and J. Dual, Simultaneous positioning of cells into two-dimensional arrays using ultrasound, *Biotechnol. Bioeng.* 97 (2007) 1335-1339.

[12] M. Wiklund, C. Günther, R. Lemor, M. Jäger, G. Fuhr and H. M. Herts, Ultrasonic standing wave manipulation technology integrated into a dielectrophoretic chip, *Lab Chip* 6 (2006) 1537-1544.

[13] K. Kwon, S. Choi, S. Lee, B. Kim, S. Lee, M. Park, P. Kim, S. Hwang and K. Suh, Label-free, microfluidic separation and enrichment of human breast cancer cells by adhesion difference, *Lab Chip* 7 (2007) 1461-1468.

[14] R. Gambari, M. Borgatti, L. Altomare, N. Manaresi, G. Medoro, A. Romani, M. Tartagni and R. Guerrieri, Applications to cancer research of "Lab-on-a-chip" devices based on dielectrophoresis (DEP), *Technol. Cancer Res. T.* 2 (2003) 31-39.

[15] J. Park, B. Kim, S. K. Choi, S. Hong, S. H. Lee and K. Lee, An efficient cell separation system using 3D-asymmetric microelectrodes, *Lab Chip* 5 (2005) 1264-1270.

[16] J. An, Y. Kim, B. Kim, S. Park, J. Park, J. Lee and S. Lee, *Proc IEEE Conf Sens 2006*, Daegu, Korea, (2007) 162-165.

[17] M. P. Hughes, *Nanoelectromechanics in Engineering and Biology*, CRC Press, Boca Raton, FL, USA, (42) 2003.

[18] H. A. Pohl, *Dielectrophoresis*, Cambridge University Press, Cambridge, UK, 34 (1978).

[19] M. dürr, J. Kentsch, T. Müller, T. Schnelle and M. Stelzle, Microdevices for manipulation and accumulation of micro- and nanoparticles by dielectrophoresis, *Electrophoresis* 24 (2003) 722-731.

[20] P. R. C. Gascoyne, X. B. Wang, Y. Huang and F. Becker, Dielectrophoretic separation of cancer cells from blood, *IEEE Trans. Ind. Appl.* 33 (1997) 670-678.

**Youngho Kim** received the B.S. degree in bioengineering from Korea University, Korea, in 2000 and the M.S. degree in electrical engineering from Korea University, Korea, in 2002. From 2002 to 2004, he worked for the Microsystem Research Center (MRC) of Korea Institute of Science and Technology (KIST), Seoul, Korea, where he engaged in national project of "Development of Micro manipulation technology"and "Development of Bio Cell Processor." From 2005 to current, he works on the system design for rare cell enrichment, high throughput sorting (HTS), and cell robot in

Nano-Bio Robotics Laboratory (NBRL) of Korea Aerospace University, Korea.

**Sang Ho Lee** received the B.S. and M.S. degrees from Korea University, Seoul, in reproductive biology, in 1978 and 1980, respectively, and the Ph.D. degree in developmental biology from University of London, London, U.K. in 1989. He worked in the MRC Experimental Embryology and Teratology Unit, St. George's Hospital Medical School, London, as a visiting scientist and nonclinical research scientist for seven years. Currently, he is the Professor of Department of Molecular and Cellular Biology, Korea University. His main interests are molecular and cellular mechanisms involved in early embryonic development and stem cell researches for cell replacement therapy.

**Byungkyu Kim** received his PhD. in mechanical engineering from the University of Wisconsin, Madison, in 1997. From 1997 to 2000, he was a research associate of CXrL (Center for X-ray Lithography) in the University of Wisconsin where he developed a computer code for thermal modeling of a mask membrane and wafer during beam exposure. From 2000 to 2005, he had worked for Microsystem Center of KIST as a principal research scientist. Currently, he is the associate professor of school of aerospace and mechanical engineering in Korea Aerospace University. His research interest includes microelectromechanical systems (MEMS) actuator, micro/nano-manipulator and bio/medical application microrobots.